Electronic supporting information available

Efficientpolymer light-emitting diodes (PLEDs) based on chiral [Pt(C^N)(N^O)]-complexes with near-infrared (NIR) luminescence and circularly polarized (CP) light

Guorui Fu, Yani He, Wentao Li, Baowen Wang, Xingqiang Lü, Hongshan He, and Wai-Yeung Wong

Supporting information

Materials and methods

All reagents were received from Sigma Aldrich and used without further purification. All solvents, unless otherwise stated were degassed and stored over 3 Å activated molecule sieves prior to use. All manipulations of air and water sensitive compounds were carried out under dry N_2 using the standard Schlenk line techniques.

Elemental analyses were performed on a Perkin-Elmer 240C elemental analyzer. Fourier Transform Infrared (FT-IR) spectra were recorded on a Nicolet Nagna-IR 550 spectrophotometer in the region 4000-400 cm^{-1} using KBr pellets. ^1H NMR spectra were recorded on a JEOL EX 400 spectrometer with $SiMe_4$ as internal standard in $CDCl_3$ at room temperature. ESI-MS was performed on a Finnigan LCQ^{DECA} XP HPLC-MS$_n$ mass spectrometer with a mass to charge (*m/z*) range of 4000 using a standard electro-spray ion source and

MeCN as the solvent. Electronic absorption spectra in the UV/Visible/NIR region were recorded with a Cary 300 UV spectrophotometer. The CD (circular dichroism) spectra were transformed from mdeg (θ) into $\Delta\varepsilon$ by using the equation:

$$\Delta\varepsilon\ (\mathrm{L/mol\cdot cm}) = \text{ellipticity (mdeg)}/[32980\times b\ (\mathrm{cm})\times c\ (\mathrm{mol/L})]$$

where b is the length of the light path and c is the concentration of the sample. Visible emission and excitation spectra were collected by a combined fluorescence lifetime and steady-state spectrometer (FLS-980, Edinburgh) with a 450 W Xe lamp. Excited-state decay times were obtained by the same spectrometer but with a μF900 Xe lamp. The luminescent quantum yield (Φ_{em}) in solution was measured with free-base tetraphenylporphyrin (Φ_r = 0.13 in toluene solution at 298 K) as the standard.[1] The solution was degassed by three freeze-pump-thaw circles. The following equation was used to calculate quantum yields:

$$\Phi_s = \Phi_r\cdot [(n_s^2\cdot A_r\cdot I_s)/(n_r^2\cdot A_s\cdot I_r)]$$

Where Φ_s is the quantum yield of the sample, Φ_r is the quantum yield of the reference, n_s is the refractive index of the sample, n_r is the refractive index of the reference, A_s and A_r are the absorbances of the sample and the reference at the wavelength of excitation (500 nm), respectively, and the I_s and I_r are the integrated areas of emission bands of the sample and the reference from 600 to 900 nm, which were recorded by a red photomultiplier tube (PMT) detector. The circularly polarized (CP) photoluminescence/electroluminescence (PL/EL) spectra were measured on a Jasco CPL-200 spectrophotometer with the "Standard" sensitivity at a 50 nm/min scan speed with 0.5 nm resolution and the respond time of 8 s. The CP PL/EL signals were presented in ΔI and no corrections were applied on the CP PL/EL spectra. $\Delta I = I_{\mathrm{L}}-I_{\mathrm{R}}$, where I_{L} and I_{R} indicate the output signals of left and right circularly polarized light. The magnitude of circular polarization in the excited state is defined as $|g_{\mathrm{lum}}|$ or $|g_{\mathrm{EL}}| = 2\times(I_L-I_R)/(I_L+I_R)$. Experimentally, the value of is calculated as $\Delta I/I$ = [ellipticity/(32980/ln10)]/unpolarized PL/EL intensity.[2] Thermal properties were characterized using thermogravimetric (TG) analyses on a NETZSCH TG 209 instrument under flowing nitrogen at a heating rate of 10 °C/min.

Synthesis of the C^N ligand Hiqbt (1-(benzo[*b*]-thiophen-2-yl)-isoquinoline)

The C^N ligand **Hiqbt** was synthesized from the improved Suzuki coupling reaction[3] of 2-Cl-isoquinoline while not 2-Br-isoquinoline with benzo[*b*]thien-2-y boronic acid. A mixture of 2-Cl-isoquinoline (0.653 g, 4.0 mmol), benzo[*b*]thien-2-y boronic acid (0.713 g, 4.0 mmol) was dissolved into absolute mixed solvents of toluene-EtOH (60 mL; V/V = 2:1) under an N_2 atmosphere. Then an aqueous solution (20 mL) of Na_2CO_3 (2 M) was added, and the mixture was degassed by an N_2 flow. Anhydrous $Pd(PPh_3)_4$ (190 mg, 0.2 mmol; 5 mol%) was added to the reaction mixture and then heated at 85 °C for 48 h. The complete consumption of reagents was monitored by TLC (Hexane/AcOEt, V/V = 9:1; $R_f = 0.25$). After cooling to RT, the organic phase was washed with brine and extracted with absolute CH_2Cl_2 (3×20 mL) three times. The combined organic phase was dried over anhydride Na_2SO_4, and further purified with flash-column chromatography on silica gel (Hexane/AcOEt, V/V = 9:1), affording to an off-white solid. Yield: 0.762 g (73%). Calc. for $C_{17}H_{11}NS$: C, 78.13; H, 4.24; N, 5.36%. Found: C, 78.05; H, 4.36; N, 5.29%. ^1H NMR (400 MHz, DMSO-d_6): δ(ppm) 8.70 (d, 1H, -Py), 8.61 (d, 1H, -Ph), 8.19 (s, 1H, -Ph), 8.11 (d, 1H, -Ph), 8.06 (m, 1H, -Ph), 8.02 (m, 1H, -Py), 7.88 (m, 2H, -Ph), 7.81 (m, 1H, -Th), 7.46 (m, 2H, -Ph).

Synthesis of the μ-chloro-bridged dimer intermediate [Pt(iqbt)(μ-Cl)]$_2$

To a mixed solvents of 2-ethoxyethanol and D. I. water (V/V = 3:1, 24 mL), **Hiqbt** (575 mg, 2.2 mmol) and **K_2PtCl_4** (415 mg, 1.0 mmol) were added, and the orange suspension was heated overnight at 80 °C under a N_2 atmosphere. After cooling to room temperature, D. I. water (30 mL) was added to the reaction mixture. The orange precipitate was filtered and washed thoroughly with D. I. water followed by isopropanol, diethyl ether and hexane, and then dried at 45°C under vacuum to constant weight. The μ-chloro-bridged dimer intermediate **[Pt(iqbt)(μ-Cl)]$_2$** was used directly for the next step without further purification. Yield: 89%.

Synthesis of the chiral Schiff-base-typed ligands *S*-HL^n (n = 1-4)

Each of the chiral Schiff-base-typed ancillary ligands ***S*-HL^n** (n = 1-4) was synthesized from the rational condensation reaction of an equimolar amount of *S*-(-)-1-phenylethylamine with one of the four salicylaldehyde derivatives (salicylaldehyde, 5-bromo-2-hydroxy-benzaldehyde*,* 5-bromo-2-hydroxy-3-methoxy-benzaldehyde or 3,5-di-*tert*-butyl-2-hydroxy-benzaldehyde) as the literature,[4] respectively.

For ***S*-HL^1**: Yield: 80%. Calc. for $C_{15}H_{15}NO$: C, 79.97; H, 6.71; N, 6.22%. Found: C, 79.91; H, 6.82; N, 6.14%. FT-IR (KBr, cm^{-1}): 3676 (w), 2980 (m), 2900 (m), 1624 (m), 1578 (w), 1493 (m), 1454 (m), 1406 (w), 1371 (w), 1346 (w), 1315 (w), 1302 (w), 1277 (m), 1236 (w), 1213 (w), 1198 (w), 1150 (w), 1124 (w), 1080 (s), 1016 (w), 970 (w), 914 (w), 850 (w), 800 (w), 758 (vs), 739 (s), 700 (s), 644 (w), 619 (w), 559 (m), 538 (m), 515 (w), 463 (m), 446 (w). ^{1}H NMR (400 MHz, DMSO-d_6): δ (ppm) 13.55 (s, 1H, -OH), 8.70 (s, 1H, -C=N), 7.47 (q, 1H, -Ph), 7.39 (m, 4H, -Ph), 7.33 (m, 1H, -Ph), 7.28 (m, 1H, -Ph), 6.91 (q, 2H, -Ph), 4.67 (q, 1H, -C*H), 1.56 (d, 3H, -

CH_3). ESI-MS (in MeCN) *m*/*z*: 226.12 (100%; $[M-H]^+$).

For ***S*-HL²**: Yield: 85%. Calc. for $C_{15}H_{14}NOBr$: C, 59.23; H, 4.64; N, 4.60%. Found: C, 59.31; H, 4.54; N, 4.67%. FT-IR (KBr, cm^{-1}): 3676 (w), 2958 (m), 2900 (m), 1627 (m), 1583 (w), 1490 (w), 1466 (m), 1450 (m), 1439 (m), 1395 (w), 1362 (m), 1342 (w), 1319 (w), 1304 (w), 1271 (w), 1250 (m), 1233 (w), 1202 (w), 1173 (w), 1134 (w), 1111 (w), 1076 (vs), 1028 (w), 976 (w), 908 (w), 880 (w), 853 (w), 827 (w), 764 (s), 731 (w), 702 (s), 644 (w), 631 (w), 594 (w), 583 (w), 538 (m), 525 (w), 501 (w). ^1H NMR (400 MHz, DMSO-d_6): δ (ppm) 13.64 (s, 1H, -OH), 8.69 (s, 1H, -CH=N), 7.71 (d, 1H, -Ph), 7.48 (q, 1H, -Ph), 7.38 (m, 4H, -Ph), 7.28 (m, 1H, -Ph), 6.87 (d, 1H, -Ph), 4.69 (q, 1H, -C*H), 1.56 (d, 3H, -CH_3). ESI-MS (in MeCN) *m*/*z*: 304.03 (100%; $[M-H]^+$).

For ***S*-HL³**: Yield: 81%. Calc. for $C_{16}H_{16}NO_2Br$: C, 57.50; H, 4.83; N, 4.19%. Found: C, 57.58; H, 4.78; N, 4.24%. FT-IR (KBr, cm^{-1}): 3649 (w), 2968 (m), 2900 (m), 1625 (m), 1570 (w), 1468 (s),1450 (m), 1439 (m), 1395 (w), 1381 (w), 1329 (w), 1250 (vs), 1099 (m), 1084 (m), 1065 (m), 1013 (w), 974 (w), 912 (w), 864 (w), 849 (w), 835 (w), 812 (w), 764 (m), 700 (s), 681 (w), 571 (w), 534 (m), 509 (w). ^1H NMR (400 MHz, DMSO-d_6): δ (ppm) 13.94 (s, 1H, -OH), 8.65 (s, 1H, -CH=N), 7.38 (m, 4H, -Ph), 7.30 (q, 1H, -Ph), 7.28 (d, 1H, -Ph), 7.16 (d, 1H, -Ph), 4.71 (q, 1H, -C*H), 3.80 (s, 3H, -OMe), 1.56 (d, 3H, -CH_3). ESI-MS (in MeCN) *m*/*z*: 334.04 (100%; $[M-H]^+$).

For ***S*-HL⁴**: Yield: 78%. Calc. for $C_{23}H_{31}NO$: C, 81.85; H, 9.26; N, 4.15%. Found: C, 81.78; H, 9.33; N, 4.20%. FT-IR (KBr, cm^{-1}): 3649 (w), 2956 (m), 2901 (m), 1628 (m), 1584 (w), 1450 (m), 1439 (m), 1395 (w), 1342 (w), 1271 (w), 1250 (m), 1233 (w), 1202 (w), 1173 (m), 1134 (w), 1111 (w), 1076 (vs), 1028 (m), 976 (w), 908 (w), 880 (w), 853 (w), 827 (m), 764 (s), 731 (w), 702 (s), 644 (w), 631 (w), 594 (w), 583 (w), 538 (m), 525 (w), 501 (w). ^{1}H NMR (400 MHz, DMSO-d_6): δ (ppm) 14.08 (s, 1H, -OH), 8.69 (s, 1H, -CH=N), 7.40 (m, 4H, -Ph), 7.32 (d, 1H, -Ph), 7.30 (d, 1H, -Ph), 7.28 (m, 1H, -Ph), 4.65 (q, 1H, -C*H), 1.57 (d, 3H, -CH_3), 1.38 (s, 9H, -$C(CH_3)_3$), 1.26 (s, 9H, -$C(CH_3)_3$). ESI-MS (in MeCN) *m/z*: 338.25 (100%; $[M-H]^+$).

Synthesis of the chiral Pt(II)-complexes [Pt(iqbt)(*S*-L^n)] (n = 1-4, 1-4)

To a solution of *μ*-chloro-bridged dimer intermediate **[Pt(iqbt)(*μ*-Cl)]$_2$** (196 mg, 0.2 mmol) in CH_2Cl_2 (10 mL), one of the chiral Schiff-base-typed ancillary ligands ***S*-HL^n** (n = 1-4; 0.6 mmol) and potassium *tert*-butoxide (*t*-BuOK; 67 mg, 0.6 mmol) were added, and each of the reaction mixture was continuously stirred at room temperature under a dry N_2 atmosphere for 24 h. After removal of the solvent under reduced pressure, the residual was purification by column chromatography on silica gel using the mixed solvents (ethyl acetate/petroleum ether (V/V = 1:15) for **1**; ethyl acetate/petroleum ether (V/V = 1:10) for **2**-**3**; CH_2Cl_2/petroleum ether (V/V = 1:4) for **4**) as the eluent, the corresponding brown-red microcrystalline product was afforded, respectively.

For [Pt(iqbt)(*S*-L^1)] (**1**): Yield: 35 mg, 26%. Calc. for $C_{32}H_{24}N_2OSPt$: C, 56.55; H, 3.56; N, 4.12%. Found: C, 56.59; H, 3.50; N, 4.17%. FT-IR (KBr, cm^{-1}): 2955 (w), 2916 (s), 2849 (m), 2361 (w), 2344 (w), 1605 (s), 1589 (m), 1547 (w), 1533 (w), 1504 (w), 1466 (w), 1441 (s), 1431 (m), 1418 (w), 1402 (w), 1379 (w), 1360 (w), 1339 (s), 1314 (w), 1277 (w), 1267 (w), 1250 (w), 1236 (w), 1213 (w), 1192 (w), 1167 (w), 1153 (w), 1130 (w), 1080 (w), 1061 (w), 1028 (w), 953 (w), 920 (w), 899 (w), 853 (w), 812 (m), 783 (w), 758 (m), 733 (vs), 712 (m), 700 (m), 683 (m), 665 (w), 621 (w), 606 (m), 567 (w), 554 (w), 540 (w), 511 (w), 488 (w), 461 (w), 440 (w). ^{1}H NMR (400 MHz, DMSO-d_6): δ (ppm) 9.02 (d, 1H, -Py), 8.68 (d, 1H, -Ph), 8.64 (s, 1H, -CH=N), 8.08 (t, 2H, -Ph), 8.03C32 (d, 1H, -Ph), 7.91 (t, 1H, -Py), 7.86 (t, 1H, -Ph), 7.73 (d, 1H, -Ph), 7.67 (t, 1H, -Ph), 7.51 (m, 2H, -Ph), 7.42 (t, 1H, -Ph), 7.22 (t, 2H, -Ph), 7.15 (t, 1H, -Ph), 7.09 (d, 2H, -Ph), 7.02 (d, 1H, -Ph), 6.66 (t, 1H, -Ph), 5.95 (q, 1H, -C*-H), 1.95 (d, 3H, -CH_3). ESI-MS (in MeCN) *m/z*: 680.13 (100%; [M-H]$^+$).

For [Pt(iqbt)(*S*-L^2)] (**2**): Yield: 46 mg, 30%. Calc. for $C_{32}H_{23}N_2OSBrPt$: C, 50.67; H, 3.06; N, 3.69%. Found: C, 50.72; H, 3.01; N, 3.76%. FT-IR (KBr, cm^{-1}): 2951 (w), 2920 (s), 2851 (m), 2361 (m), 2342 (w), 1611 (s), 1545 (w), 1518 (w), 1503 (w), 1442 (s), 1429 (s), 1418 (s), 1375 (m), 1346 (m), 1321 (m), 1288 (m), 1249 (m), 1173 (m), 1150 (w), 1132 (m), 1113 (w), 1070 (m), 1051 (w), 1011 (w), 999 (w), 970 (w), 935 (w), 922 (m), 866 (w), 856 (m), 824 (s), 787 (w), 762 (s), 745 (m), 735 (m), 700 (s), 683 (vs), 664 (m), 644 (m), 600 (w), 565 (w), 546 (m), 534 (w), 501 (w), 457 (w), 438 (w). ^{1}H NMR (400 MHz, DMSO-d_6): δ (ppm) 8.95 (d, 1H, -Py), 8.70 (s, 1H, -CH=N), 8.68 (s, 1H, -Ph), 8.08 (t, 2H, -Ph), 8.00 (d, 1H, -Ph), 7.93 (t, 1H, -Py),7.90 (d, 1H, -Ph), 7.86 (d, 1H, -Ph), 7.73 (d, 1H, -Ph),7.54 (m, 2H, -Ph), 7.49 (q, 1H, -Ph), 7.23 (t, 2H, -Ph), 7.16 (t, 1H, -Ph), 7.07 (d, 2H, -Ph), 6.99 (d, 1H, -Ph), 5.94 (q, 1H, -C*-H), 1.94 (d, 3H, -CH_3). ESI-MS (in MeCN) *m/z*: 759.04 (100%; [M-H]$^+$).

For [Pt(iqbt)(*S*-L^3)] (**3**): Yield: 32 mg, 20%. Calc. for $C_{33}H_{25}N_2O_2SBrPt$: C, 50.26; H, 3.20; N, 3.55%. Found: C, 50.31; H, 3.25; N, 3.61%. FT-IR (KBr, cm^{-1}): 2951 (w), 2916 (m), 2849 (m), 2361 (m), 2342 (m), 1627 (w), 1585 (m), 1558 (w), 1533 (m), 1506 (w), 1464 (s), 1439 (s), 1418 (s), 1366 (m), 1339 (m), 1310 (w), 1290 (w), 1271 (m), 1254 (m), 1236 (s), 1198 (m), 1188 (m), 1169 (m), 1150 (m), 1126 (s), 1097 (s), 1074 (s), 1049 (s), 1030 (s), 1007 (m), 995 (s), 970 (m), 953 (m), 916 (w), 866 (w), 854 (m), 843 (m), 829 (m), 814 (s), 781 (s), 754 (s), 733 (vs), 702 (s), 681 (s), 664 (m), 619 (m), 604 (m), 563 (s), 544 (w), 505 (w), 470 (w), 438 (w). ^{1}H NMR (400 MHz, DMSO-d_6): δ (ppm) 9.11 (d, 1H, -Py), 8.68 (d, 1H, -Ph), 8.65 (s, 1H, -CH=N), 8.07 (q, 2H, -Ph), 8.01 (d, 1H, -Ph), 7.93 (t, 1H, -Py), 7.87 (t, 1H, -Ph), 7.76 (d, 1H, -Py), 7.67 (m, 1H, -Ph), 7.52 (m, 2H, -Ph), 7.48 (q, 1H, -Ph), 7.23 (t, 2H, -Ph), 7.15 (q, 2H, -Ph), 7.08 (d, 1H, -Ph), 5.96 (q, 1H, -C*-H), 3.88 (s, 3H, -OMe), 1.94 (d, 3H, -CH_3). ESI-MS (in MeCN) *m/z*: 789.05 (100%; $[M-H]^+$).

For [Pt(iqbt)(*S*-L^4)] (**4**): Yield: 31 mg, 20%. Calc. for $C_{38}H_{40}N_2OSPt$: C, 59.44; H, 5.25; N, 3.65%. Found: C, 59.49; H, 5.21; N, 3.61%. FT-IR (KBr, cm^{-1}): 2951 (w), 2901 (w), 2866 (w), 2361 (m), 2344 (w), 1609 (s), 1543 (m), 1528 (m), 1504 (w), 1456 (m), 1441 (s), 1429 (s), 1418 (s), 1393 (m), 1360 (m), 1342 (m), 1325 (m), 1271 (m), 1254 (s), 1234 (m), 1198 (w), 1169 (m), 1148 (w), 1130 (w), 1070 (w), 1028 (w), 1011 (w), 972 (w), 947 (w), 922 (w), 907 (w), 856 (m), 835 (m), 810 (m), 783 (m), 756 (m), 733 (s), 708 (w), 696 (m), 685 (vs), 663 (w), 637 (w), 621 (w), 604 (w), 581 (w), 565 (w), 546 (w), 532 (w), 503 (w), 474 (m), 436 (w). ^{1}H NMR (400 MHz, DMSO-d_6): δ (ppm) 9.18 (d, 1H, -Py), 8.72 (s, 1H, -CH=N), 8.70 (s, 1H, -Ph), 8.09 (t, 2H, -Ph), 8.05 (s, 1H, -Ph), 7.93 (t, 1H, -Py), 7.88 (t, 1H, -Ph), 7.77 (d, 1H, -Py), 7.52 (m, 2H, -Ph), 7.48 (q, 2H, -Ph), 7.21 (t, 2H, -Ph), 7.15 (t, 3H, -Ph), 5.95 (q, 1H, -C*-H), 1.98 (d, 3H, -CH_3), 1.53 (s, 9H, -$C(CH_3)_3$), 1.33 (s, 9H, -$C(CH_3)_3$). ESI-MS (in MeCN) *m/z*: 768.26 (100%; $[M-H]^+$).

X-ray crystallography

Single crystals for the chiral Pt(II)-complex [Pt(iqbt)(*S*-L^3)] (**3**) of suitable dimensions were mounted onto thin glass fibers. All the intensity data were collected on a Bruker SMART CCD diffractometer (Mo-Kα radiation and λ = 0.71073 Å) in Φ and ω scan modes. Structures were solved by Direct methods followed by difference Fourier syntheses, and then refined by full-matrix least-squares techniques against F^2 using SHELXTL.[5] All other non-hydrogen atoms were refined with anisotropic thermal parameters. Absorption corrections were applied using SADABS.[6] All hydrogen atoms were placed in calculated positions and refined isotropically using a riding model. Crystallographic data, relevant atomic distances and bond angles for chiral Pt(II)-complex [Pt(iqbt)(*S*-L^3)] (**3**) are presented in Tables S2-3, respectively. CCDC number 1941079 for chiral Pt(II)-complex[Pt(iqbt)(*S*-L^3)] (**3**).

Electronic structure calculations

To gain further insight into the photophysical and electrochemical characteristics of the chiral Pt(II)-complexes **1**-**4**, theoretical studies on their electronic structures were carried out using density functional theory (DFT) and time-dependent DFT (TD-DFT) methods. Each of their molecular structures was optimized at the ground state (S_0) in the gas phase. DFT calculations were conducted with the popular B3LYP functional theory. The 6-31G (d, p) basis set was applied for C, H, N, O, S, Br atoms, while effective core potentials employed for Pt atom were based on a LanL2DZ basis set.[7-8] The excited states' energies of the Pt(II)-complex were computed by TD-DFT based on all the ground-state (S_0) geometries. Additionally, the natural transition orbital (NTO) was analyzed for $S_0 \rightarrow T_1$ excitation based on the first triplet state (T_1) geometries optimized by UB3LYP. All calculations were carried out with Gaussian 09, Revision D.01 software package.[9] The electron density diagrams of molecular orbitals were obtained with the ChemOffice 2010 graphics program.

Cyclic voltammetry (CV) measurement

CV measurement was performed on a computer-controlled EG&G Potentiostat/Galvanostat model 283 at RT with a conventional three-electrode cell using a an Ag/$AgNO_3$ (0.1 M) reference electrode, Pt carbon working electrode of 2 mm in diameter, and a platinum wire counter electrode. CV of the sample was performed in nitrogen-saturated dichloromethane containing 0.1 M Bu_4NPF_6 as supporting electrolyte. The CV was measured at a scan rate of 100 $mV \cdot s^{-1}$. The HOMO and the LUMO energy levels of each complex are calculated according to the following equations,[10] $E_{HOMO} = -(E_{OX}{}^{on} + 4.8)$ eV, $E_{LUMO} = -(E_{red}{}^{on} + 4.8)$ eV, and where $E_{OX}{}^{on}$ is the recorded onset oxidation potential of the complex, and $E_{red}{}^{on}$ is the recorded onset reduction potential of the complex. The HOMO and LUMO energy levels for the other used materials were obtained from the literatures.[11]

CP-NIR-PLEDs' fabrication and testing

Each of the series of **CP-NIR-PLEDs-A/B** was fabricated on ITO (Indium tin oxide) coated glass substrates with a sheet resistance of 20 Ω per square. Patterned ITO coated glass substrates were washed with acetone, detergent, D. I. water and isopropanol in an ultrasonic bath. After being exposed under oxygen plasma for 20 min, PEDOT:PSS (poly(3,4-ethylenedioxythiophene):poly(styrenesulfonate) from water solution was spin-coated (at 2000 rpm) on the substrate and followed by drying in a vacuum oven at 140 °C for 20 min, giving a film of 40 nm thickness. The chlorobenzene solution (20 mg/mL) of the mixture of PVK (poly(*N*-vinylcarbazole; $M_n = 2.5 \times 10^4$ g/mol, PDI = $M_w/M_n = 2.8$), PBD(2-(4-*tert*-butylphenyl)-5-(4-biphenylyl)-1,3,4-oxadiazole) and one of the chiral Pt(II)-complexes

[Pt(iqbt)(S-L^n)] (**1**-**4**) as the emitting layer was prepared under an N_2atmosphere and spin-coated (at 4000 rpm) on the PEDOT:PSS layer with a thickness of 100 nm. The TPBi (2,2',2''-(1,3,5-benzenetriyl)*tris*-(1-phenyl-1*H*-benzimidazole)) layer (40 nm) and/or the BCP (2,9-dimethyl-4,7-diphenyl-1,10-phenanthroline) layer (10 nm) were thermally deposited onto the emitting layer. Finally, a thin layer (1 nm) of LiF followed by 100 nm thickness Al capping layer was deposited onto the substrate under vacuum of 5×10^{-6} Pa. Current density-voltage (*J*-*V*) characteristics were collected using a Keithley 2400 source meter equipped with a calibrated silicon photodiode. The NIR EL irradiance (L_e) was measured through a M6100 Spectra Scan spectrometer. The eternal quantum efficiencies (EQEs) of the NIR emission were obtained by measuring the irradiance in the forward direction and assuming the eternal emission profile to Lambertian.

References

1. J. H. Palmer, A. C. Durrell, Z. Gross, J. R. Winkler, H. B. Gray, *J. Am. Chem. Soc.* 2010, **132**, 9230-9231.
2. Y. Nakano, F. Ichiyanagi, M. Naito, Y. G. Yang, M. Fujiki, M. *Chem. Commun.* 2012, **48**, 6636-6638.
3. G. N. Li, Y. Zou, Y. D. Yang, J. Liang, F. Cui, T. Zheng, H. Xie, Z. G. Niu, *J. Fluoresc* 2014, **24**, 1545-1552.
4. S. Kesarkar, W. Mróz, M. Penconi, M. Pasini, S. Destri, M. Cazzaniga, D. Ceresoli, P. R. Mussini, C. Baldoli, U. Giovanella, A. Bossi, A. *Angew. Chem. Int. Ed.* 2016, **55**, 2714-2718.
5. G. M. Sheldrick, *SHELXL-97*, *Program for Crystal Structure Refinement*, University of

Göttingen, Göttingen, Germany, 1997.

6. G. M. Sheldrick, G. M. *SADABS*, University of Göttingen, Göttingen, Germany, 1996.
7. W. R. Wadt, P. J. Hay,*J. Chem. Phys.* 1985, **82**, 284-298.
8. P. J. Hay, W. R. Wadt, *J. Chem. Phys.* 1985, **82**, 299-310.
9. M. J. Frisch, G. W. Trucks, H. B. Schlegel, G. E. Scuseria, M. A. Robb, J. R. Cheeseman, G. Scalmani, V. Barone, B. Mennucci, G. A. Petersson, H. Nakatsuji, M. Caricato, X. Li, H. P. Hratchian, A. F. Izmaylov, J. Bloino, G. Zheng, J. L. Sonnenberg, M. Hada, M. Ehara, K. Toyota, R. Fukuda, J. Hasegawa, M. Ishida, T. Nakajima, Y. Honda, O. Kitao, H. Nakai, T. Vreven, J. A. Montgomery, Jr., J. E. Peralta, F. Ogliaro, M. Bearpark, J. J. Heyd, E. Brothers, K. N. Kudin, V. N. Staroverov, R. Kobayashi, J. Normand, K. Raghavachari, A. Rendell, J. C. Burant, S. S. Iyengar, J. Tomasi, M. Cossi, N. Rega, J. M. Millam, M. Klene, J. E. Knox, J. B. Cross, V. Bakken, C. Adamo, J. Jaramillo, R. Gomperts, R. E. Stratmann, O. Yazyev, A. J. Austin, R. Cammi, C. Pomelli, J. W. Ochterski, R. L. Martin, K. Morokuma, V. G. Zakrzewski, G. A. Voth, P. Salvador, J. J. Dannenberg, S. Dapprich, A. D. Daniels, Ö. Farkas, J. B. Foresman, J. V. Ortiz, J. Cioslowski, D. J. Fox, Gaussian 09, Revision D.01, Gaussian, Inc., Wallingford CT, 2009.
10. H. Y. Chen, C. T. Chen, Chen, C. T. *Macromolecules* 2010, **43**, 3613-3623.
11. E. Zysman-Colman, S. S. Ghosh, G. Xie, S. Varghese, M. Chowdhury, N. Sharma, D. B. Cordes, A. M. Z. Slawin, I. D. W. Samuel, *ACS Appl. Mater. & Interfaces* 2016, **8**, 9247-9253.

Table S1. The coordination bond lengths (Å) of the chiral Pt(II)-complex [Pt(iqbt)(*S*-L^n)] (n = 1-4, **1**-**4**) based on the TD-DFT calculations

Complexes	Pt(1)-C(11)	Pt(1)-N(1)	Pt(1)-N(2)	Pt(1)-O(1)/O(2)
1	**2.00841**	**2.06398**	**2.06015**	**2.10565**
2	**1.99421**	**2.06234**	**2.05599**	**2.11856**
3	**2.00740**	**2.06532**	**2.05723**	**2.10211**
4	**2.00438**	**2.05585**	**2.06706**	**2.12124**

Table S2. The crystallographic data for the chiral Pt(II)-complex [Pt(iqbt)(*S*-L^3)] (**3**)

Compound	**[Pt(iqbt)(*S*-L^3)] (3)**
Empirical formula	$C_{33}H_{25}N_2O_2SBrPt$
Formula weight	**788.61**
Crystal system	**triclinic**
Space group	***P1***
***a*/Å**	**6.608(3)**
***b*/Å**	**9.229(4)**
***c*/Å**	**12.393(7)**
***α*/°**	**105.413(9)**
***β*/°**	**95.039(9)**
***γ*/°**	**104.004(6)**
***V*/Å³**	**697.5(6)**
Z	**1**
***ρ*/g·cm⁻³**	**1.877**
Crystal size/mm	**0.22× 0.18× 0.17**
***μ*(Mo-Kα)/mm⁻¹**	**6.571**
Data/restraints/parameters	**3103/45/361**
Quality-of-fit indicator	**1.053**
No. unique reflections	**3103**
No. observed reflections	**3667**
Final *R* indices [$I > 2\sigma(I)$]	$R_1 = 0.0743$
	$wR_2 = 0.1860$
***R* indices (all data)**	$R_1 = 0.0748$
	$wR_2 = 0.1868$

Table S3. The relevant atomic distances (Å) and bond angles (°) for the chiral Pt(II)-complex [Pt(iqbt)(*S*-L^3)] (**3**)

Compound	**Pt(iqbt)(*S*-L^3)] (3)**		
Pt(1)-C(11)	**2.07(3)**	**Pt(1)-N(1)**	**1.99(3)**
Pt(1)-N(2)	**2.06(3)**	**Pt(1)-O(2)**	**1.99(2)**
C(11)-Pt(1)-N(1)	**83.3(14)**	**C(11)-Pt(1)-N(2)**	**99.9(11)**
C(11)-Pt(1)-O(2)	**167.0(10)**		

Table S4. Photophysical and electrochemical properties of the four chiral [Pt(iqbt)(*S*-L^n)] (n = 1-4, **1**-**4**) in degassed solution at RT or 77 K

Comp.	Absorption	Em (RT)[a]					Em (77 K)		Em (RT)[b]	Energy level[c,d]	
	λ_{abs} [nm]	λ_{em} [nm]	τ [μs]	Φ	k_r [10^5 s^{-1}]	k_{nr} [10^5 s^{-1}]	λ_{em} [nm]	τ [μs]	λ_{em} [nm]	HOMO (eV)	LUMO (eV)
1	227, 328, 376, 430, 518	731, 807 (sh)	0.88	0.13	1.48	9.89	744, 808 (sh)	1.04	725, 795 (sh)	-5.63 (-4.98)	-2.86 (-2.07)
2	229, 329, 376, 439, 518	729, 808 (sh)	1.02	0.21	2.10	7.75	743, 808 (sh)	1.34	727, 799 (sh)	-5.66 (-5.05)	-2.95 (-2.19)
3	228, 329, 375, 441, 519	730, 806 (sh)	0.96	0.16	1.67	8.75	741 803 (sh)	1.27	741, 784 (sh)	-5.64 (-4.94)	-2.94 (-2.11)
4	226, 320, 378, 440, 521	731, 804 (sh)	0.85	0.14	1.65	10.11	745, 807 (sh)	1.01	751, 801 (sh)	-5.60 (-4.89)	-2.88 (-2.09)

[a] In degassed CH_2Cl_2 solution; rate constant k_r and k_{nr} are calculated using the equations $k_r = \Phi_{em}/\tau$ and $k_{nr} = (1-\Phi_{em})/\tau$ on the assumption that $\Phi_{ISC} = 1$ (ISC = intersystem crossing). [b] In solid state; [c,d] HOMO and LUMO levels are obtained from electrochemical determination and theoretical calculation, respectively.

Table S5. The TD-DFT results for the chiral Pt(II)-complex [Pt(iqbt)(*S*-L^n)] (**1**-**4**) based on their optimized S_0 geometries

Comp.	**MO**	**Contribn of metal $d_\pi$and π orbitals of ligand to MOs (%)**			**Main confign of $S_0 \rightarrow S_n$ excitation, λ_{cal}(nm)/f** [a]	**Main confign of $S_0 \rightarrow T_1$ excitation, λ_{cal}(nm)**[a]
		Pt	**iqbt**	***S*-L^n**		
1	**L+1**	**2.76**	**5.42**	**91.82**	**S_1: H→L (97.30), 513.7, 0.1273**	**H → L (71.34); H-1 → L (23.38), 707.0**
	L	**5.85**	**90.54**	**3.61**	**S_2: H-1 → L (95.92), 429.8, 0.1148**	
	H	**17.74**	**43.90**	**38.36**		
	H-1	**6.14**	**47.94**	**45.92**		
2	**L+1**	**3.11**	**3.85**	**93.04**	**S_1: H→L (97.45), 523.6, 0.1253**	**H → L (66.06); H-1 → L (28.69), 710.5**
	L	**5.91**	**90.51**	**3.58**	**S_2: H-1→ L (95.60), 436.2, 0.1039**	
	H	**16.52**	**35.67**	**47.81**		
	H-1	**5.32**	**53.47**	**41.21**		
3	**L+1**	**2.99**	**5.04**	**91.97**	**S_1: H→L (97.74), 526.0, 0.1095**	**H → L (55.30); H-1→ L (39.01),707.3**
	L	**5.83**	**90.40**	**3.77**	**S_2: H-1→ L (96.16), 444.6, 0.1146**	
	H	**13.31**	**26.82**	**59.87**		
	H-1	**5.69**	**62.32**	**31.99**		
4	**L+1**	**2.77**	**7.03**	**90.20**	**S_1: H→L (97.78), 532.1, 0.1142**	**H → L (56.29); H-1→ L (38.61), 707.4**
	L	**5.90**	**90.68**	**3.42**	**S_2: H-1→ L (95.52), 439.3, 0.1142**	
	H	**14.03**	**25.49**	**60.48**		
	H-1	**6.66**	**63.88**	**29.46**		

[a] H→ L denotes the transition from HOMO to LUMO. λ_{cal}, and *f* denote the calculated emission wavelength, and oscillator strength, respectively. The oscillator strength of $S_0 \rightarrow T_1$ is zero owing to the spin-forbidden character of the singlet-triplet transition under TD-DFT calculations in the Gaussian program with no consideration of spin-orbital coupling.

Table S6. The NTO results for the chiral Pt(II)-complex [Pt(iqbt)(*S*-L^n)] (**1**-**4**) based on their optimized T_1 geometries

complex	**NTO**[a]	**Contribution of metal d$_\pi$ and π orbitals of ligand to NTOs (%)**		
		Pt	**iqbt**	***S*-L^n**
1	**H**	**12.97**	**81.70**	**5.33**
	P	**6.08**	**91.76**	**2.16**
2	**H**	**13.79**	**79.71**	**6.50**
	P	**6.21**	**91.65**	**2.14**
3	**H**	**12.48**	**80.74**	**6.78**
	P	**6.03**	**91.63**	**2.34**
4	**H**	**13.44**	**78.68**	**7.88**
	P	**6.18**	**91.45**	**2.37**

[a] H and P denote NTO hole and particle orbitals, respectively

Table S7. Device characteristics of the **CP-NIR-PLED-A/B** based on the chiral Pt(II)-complexes **1-4**

Device	λ_{EL} [nm]	V_{on} [V]	L_e^{max}	η_{EQE}^{max} [%]	g_{EL}^{Max}
CP-NIR-PLED-A-1	**732**	**13.5**	**0.023**	**0.44 (16.0 V)**	**-2.21×10^{-3} (732 nm)**
CP-NIR-PLED-A-2	**732**	**10.5**	**0.081**	**0.87 (12.0 V)**	**-1.77×10^{-3} (732nm)**
CP-NIR-PLED-A-3	**732**	**13.5**	**0.017**	**0.49 (16.0 V)**	**-1.93×10^{-3} (732 nm)**
CP-NIR-PLED-A-4	**732**	**13.5**	**0.007**	**0.48 (18.0 V)**	**-2.73×10^{-3} (732 nm)**
CP-NIR-PLED-B-2	**732**	**6.0**	**0.248**	**0.93 (11.0 V)**	**-1.77×10^{-3} (732 nm)**

Figure S1. The ^{1}H NMR spectra of the chiral Pt(II)-complexes [Pt(iqbt)(*S*-L^n)](**1**-**4**) in DMSO-d_6 at RT.

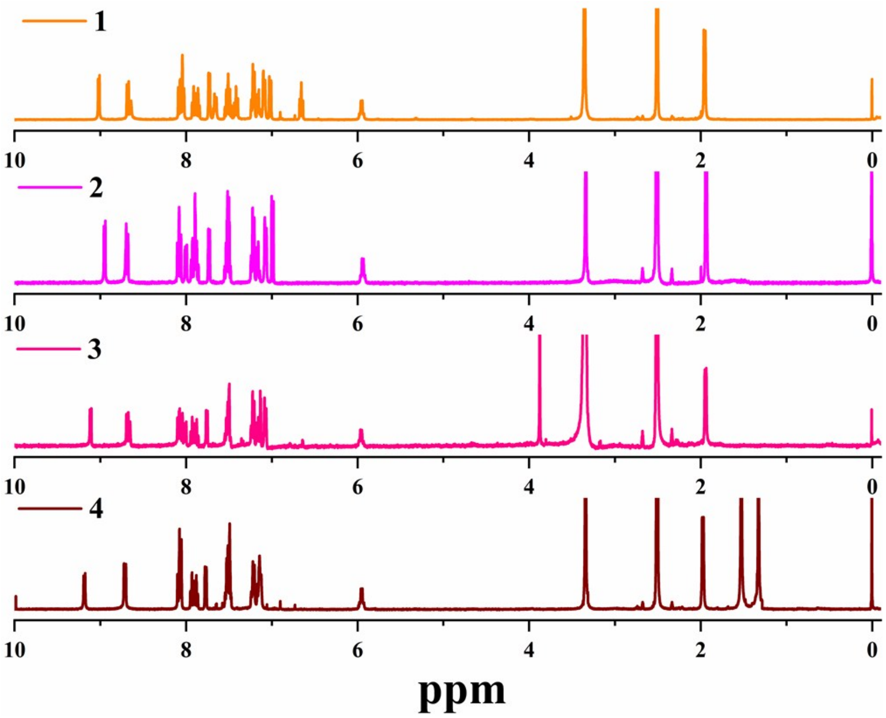

Figure S2. The ^{1}H NMR spectra of the C^N main ligand **Hiqbt** and the chiral Schiff-base-typed ancillary ligands ***S*-HL^n** (n = **1**-**4**) in DMSO-d_6 at RT.

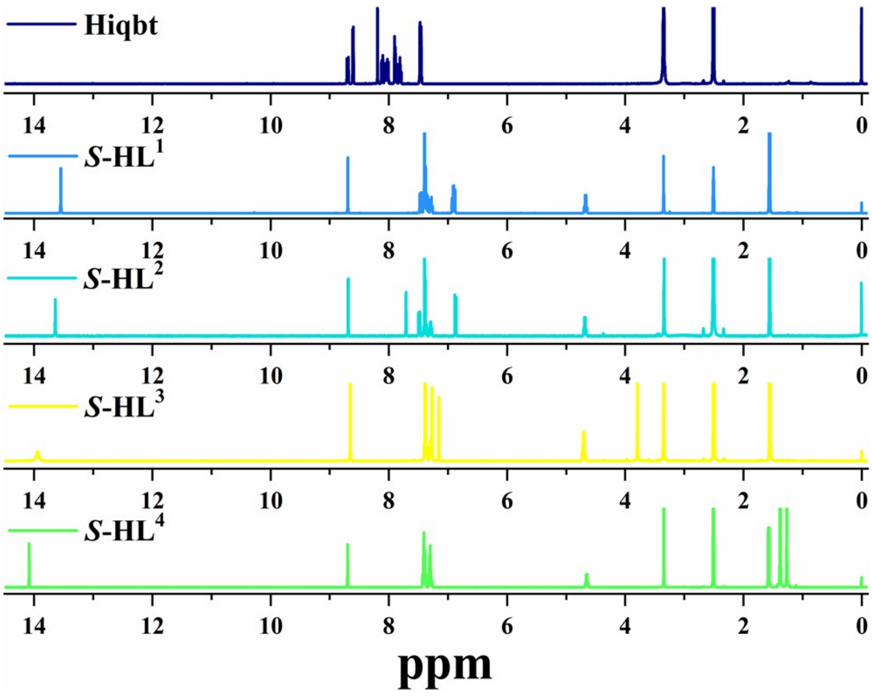

Figure S3. The TG curves for the chiral Ir(III)-complexes [Pt(iqbt)(*S*-L^n)](**1**-**4**).

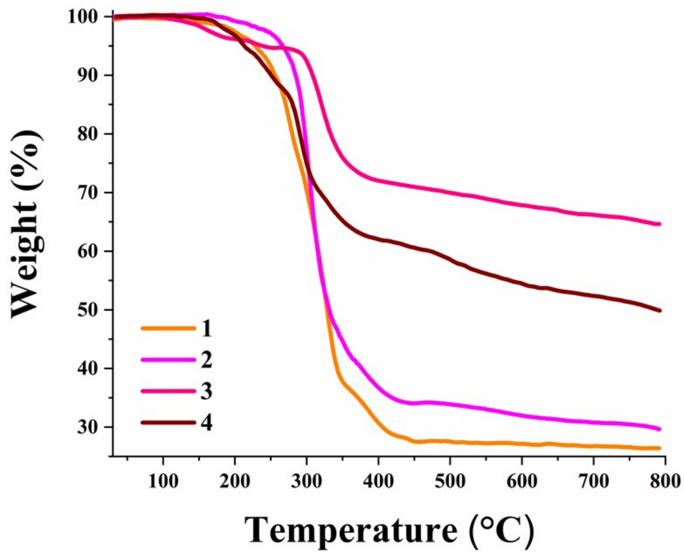

Figure S4. The polymer chain network of the chiral Pt(II)-complex [Pt(iqbt)(*S*-L^3)](**3**) with complementary intermolecular interactions (3.566(2) Å of π···π, 3.791(2) Å of π···Pt and 3.710(30) Å of C18-H18···π).

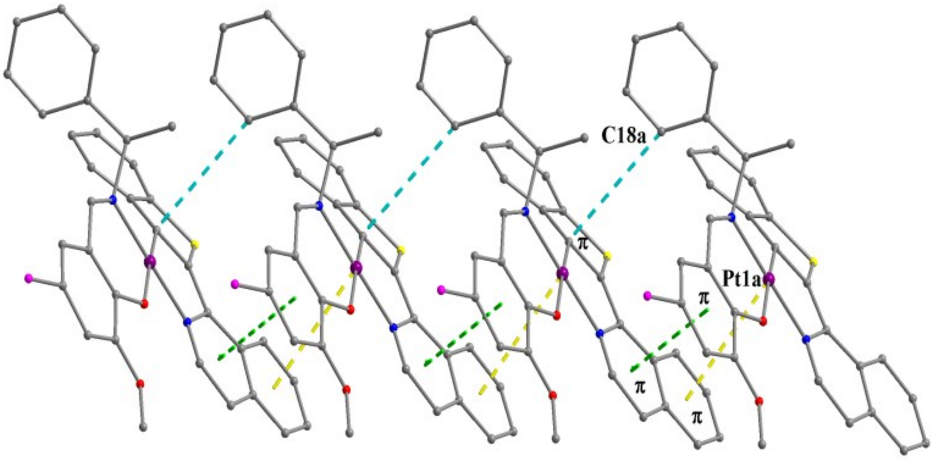

Figure S5. The normalized UV-visible absorption (down) and CD spectra (up) of the chiral Schiff-base-typed ligands ***S*-HL^n** (n = 1-4) or the ligand **Hiqbt** in degassed CH_2Cl_2 solution at RT.

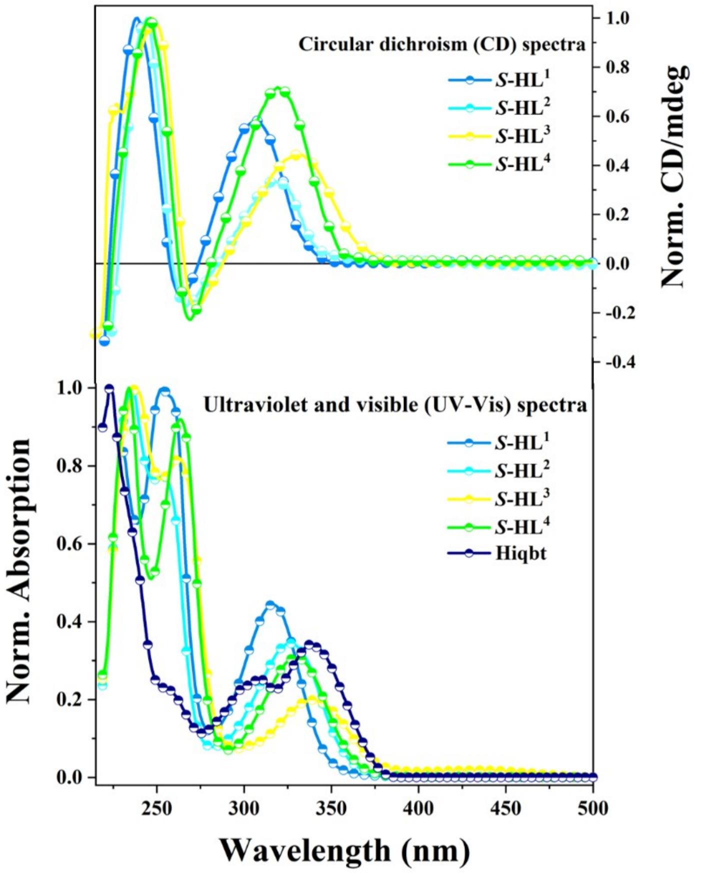

Figure S6. The normalized CD spectra ofthe chiral Pt(II)-complexes [Pt(iqbt)(*S*-L^n) (**1**-**4**) in degassed CH_2Cl_2 solution at RT.

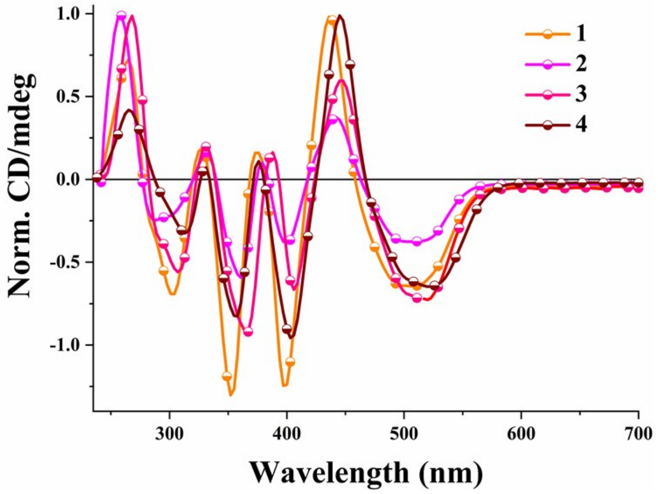

Figure S7. The normalized emission and excitation spectra of the chiral Schiff-base-typed ancillary ligands ***S*-HL^n** (n = 1-4) in degassed CH_2Cl_2 solution at RT.

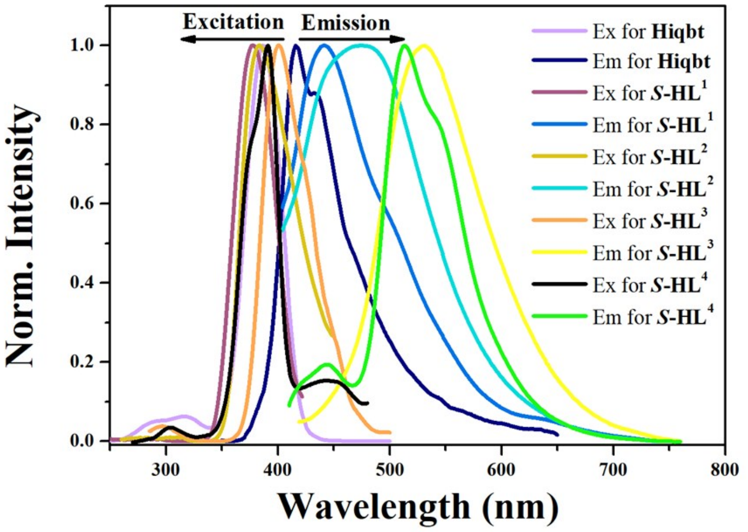

Figure S8. The normalized emission and excitation spectra of the chiral Pt(II)-complexes [Pt(iqbt)(*S*-L^n) (**1**-**4**) in CH_2Cl_2 solution at RT or 77 K.

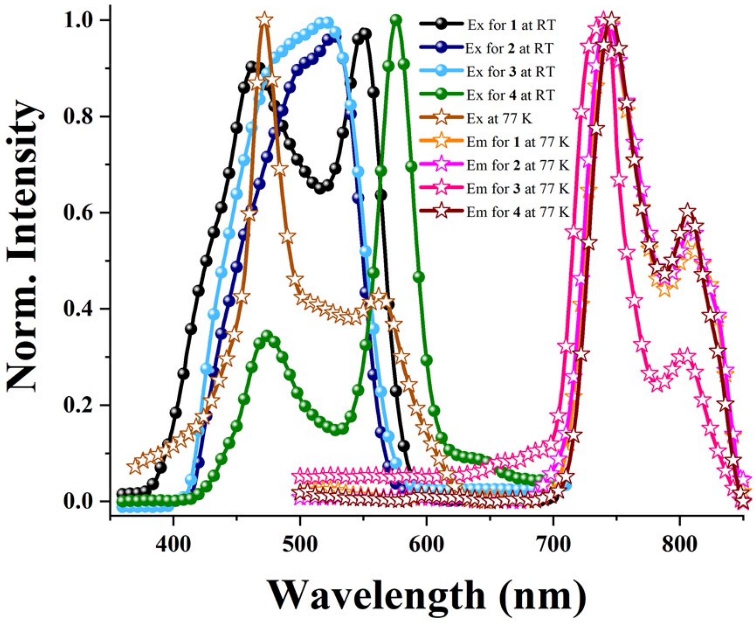

Figure S9. The normalized emission spectra of the chiral Pt(II)-complexes [Pt(iqbt)(*S*-L^n) (**1**-**4**) in solid-state at RT.

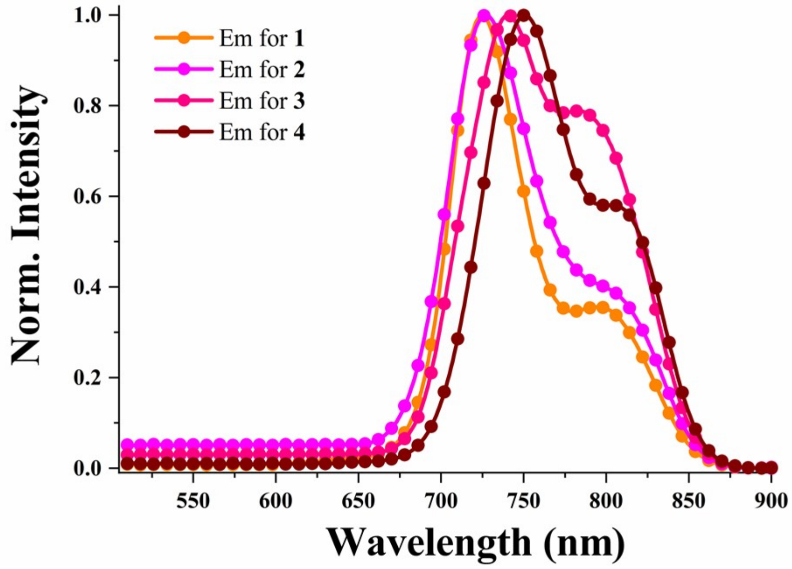

Figure S10. The HOMOs and LUMOs patterns for the chiral Pt(II)-complexes [Pt(iqbt)(*S*-L^n)] (**1**-**4**) based on their optimized S_0 geometries.

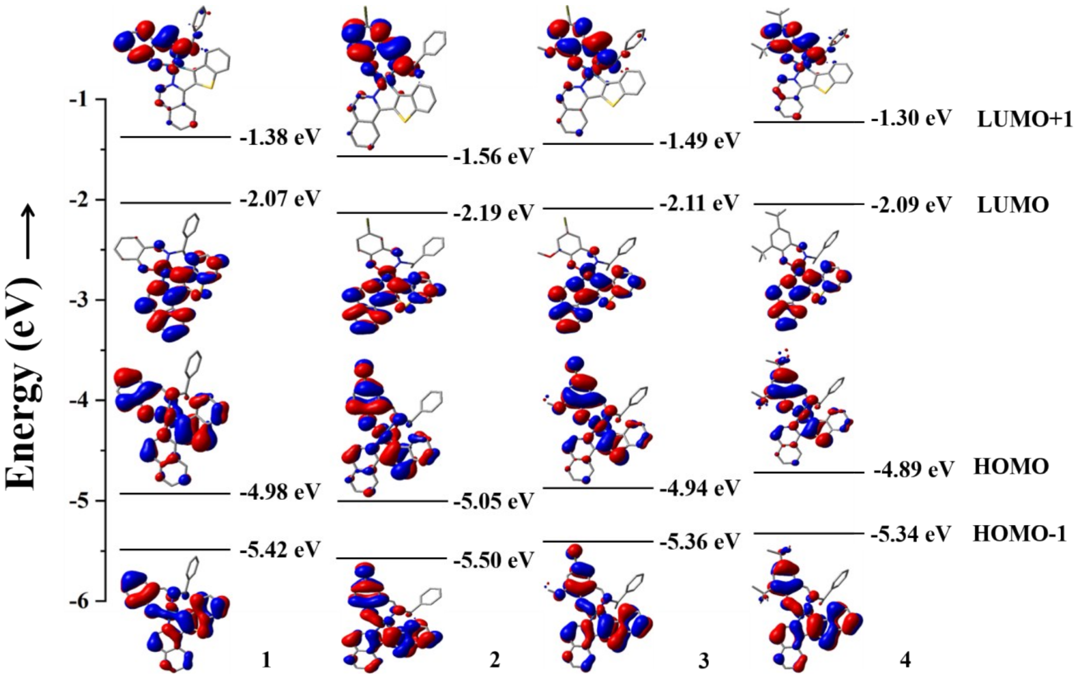

Figure S11. The NTO patterns for $S_0 \rightarrow T_1$ excitation for the chiral Pt(II)-complexes [Pt(iqbt)(*S*-L^n)] (**1**-**4**) based on their optimized T_1 geometries.

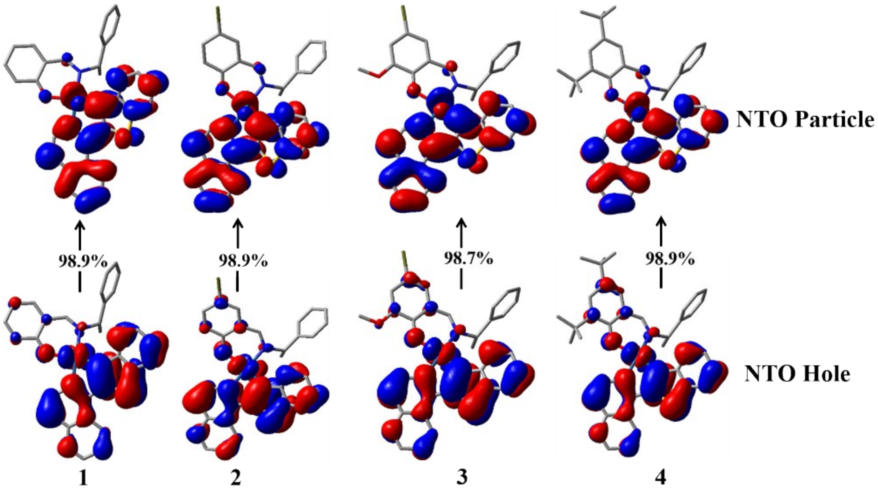

Figure S12. The CV curves of the chiral Pt(II)-complexes [Pt(iqbt)(*S*-L^n)](**1**-**4**) recorded *versus* Fc$^+$/Fc in degassed MeCN solution at room temperature under a N_2 atmosphere (scan rate = 100 mV/s).

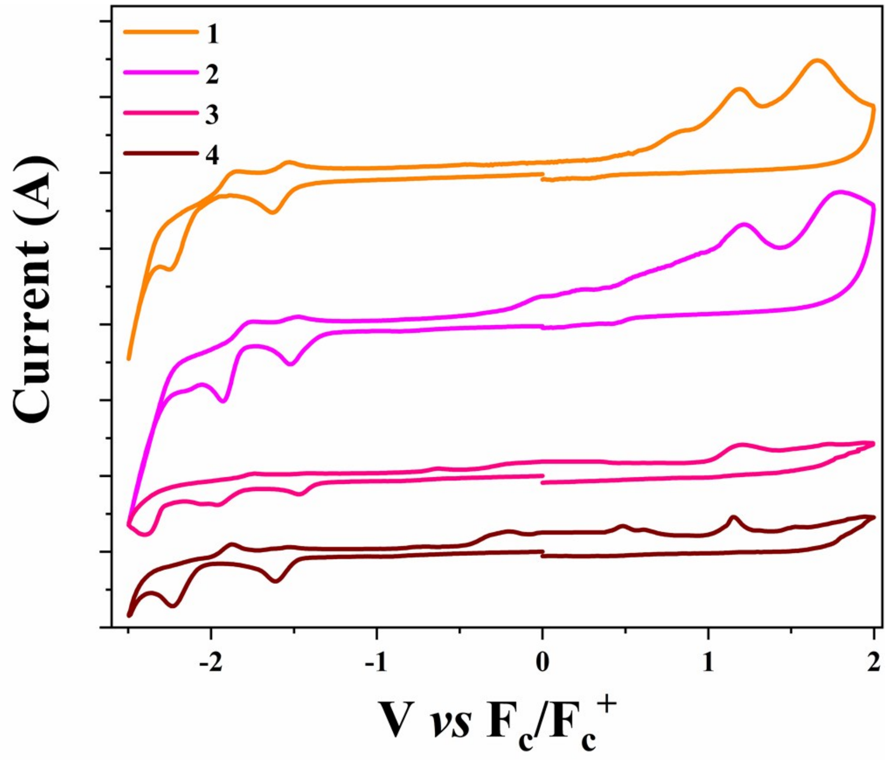

Figure S13. The Electroluminescent spectra of **CP-NIR-PLEDs-A/B** based on the four chiral Pt(II)-complexes [Pt(iqbt)(*S*-L^n)] (**1**-**4**) with BCP or not.